Narrow-linewidth middle-infrared ZnGeP$_2$ optical parametric oscillator

F. Ganikhanov,* T. Caughey, and K. L. Vodopyanov[†]

INRAD, Inc., 181 Legrand Avenue, Northvale, New Jersey 07647

We report a narrow-linewidth ZnGeP$_2$ (ZGP) optical parametric oscillator (OPO). It employs a *Q*-switched Nd:YAG-laser-pumped LiNbO$_3$ OPO with an output at $\lambda = 2.55$ μm that is used as a pump for the ZGP OPO. With the singly resonant type II ZGP OPO cavity containing a diffraction grating and a Si etalon, we achieved mid-IR tunability from 3.7 to 8 μm with an output linewidth of ~0.1 cm^{-1}, corresponding to ~3 axial cavity modes. We have also demonstrated that such a narrow-linewidth OPO can be achieved with a fairly broad-band (~15 cm^{-1}) pump.   © 2001 Optical Society of America

OCIS codes: 190.0190, 190.4970, 140.3070.

1. INTRODUCTION

A narrow–band, widely tunable mid-IR source of coherent light in the 3–12 μm wavelength range is of great appeal because of its potential for use in molecular detection systems that are sensitive and species specific. In recent years, zinc germanim phosphide (ZGP) has become the most promising nonlinear crystal for high average power (up to 10 W) and high peak power (up to 1 MW) frequency conversion in the mid-IR range beyond $\lambda = 5$ μm. The main virtues of ZGP are a high nonlinear coefficient ($d_{36} = 75$ pm/V), a high damage threshold, and high thermal conductivity.[1] In addition, progress in ZGP crystal growth in the last decade has resulted in dramatic improvement in the crystal's optical transmission:[2,3] for example, ZGP transmits light ($\alpha < 1$ cm^{-1}) from 1.3 to 11.1 μm and has very low losses (<0.01 cm^{-1}) between 3 and 8 μm. As a result, efficient operation of ZGP optical parametric oscillators (OPOs) and generators (OPGs) has been demonstrated with nanosecond[4–10] and picosecond–femtosecond[11,12] pulsed systems.

For efficient frequency conversion, ZGP has to be pumped at wavelengths where the linear absorption of the crystal is low. A number of approaches have been used in previous research, including direct OPO pumping by an Er (2.8–2.9 μm)[4,9] or a Ho (2–2.1 μm) laser,[5] cascaded laser pumping[11] (e.g., with 1.9-μm Tm-laser-pumped 2.1-μm Ho laser), or tandem OPO setups.[6–8]

From the standpoint of spectroscopic applications, to achieve sufficient discrimination in detecting molecular species at atmospheric pressure (e.g., CO, CO$_2$, H$_2$O, CH$_4$, NO, N$_2$O), a spectral resolution of the order of 0.1 cm^{-1} or better is desired. Although most of the previous studies on ZGP OPO were focused on obtaining high average power and broad tunability in the mid-IR, experimental work addressing a narrow-linewidth performance ($\leqslant 1$ cm^{-1}) have not been reported so far: the spectral width of tunable mid-IR pulses obtained from ZGP OPO was typically 2–5 cm^{-1} far from degeneracy and 100–200 cm^{-1} near degeneracy.

In this paper, we demonstrate a narrow-linewidth (~0.1 cm^{-1}) ZGP OPO. As a driving source, we employ a *Q*-switched Nd:YAG 1.06-μm laser with a 10-Hz repetition rate, whose wavelength is converted in a LiNbO$_3$ OPO to $\lambda \approx 2.55$ μm for pumping the type II ZGP OPO (a tandem OPO approach). The optical layout of the system is shown in some detail in Fig. 1.

2. MAXIMUM ACCEPTED BANDWIDTH OF THE PUMP

In a singly resonant OPO (SRO), a narrow linewidth can be achieved at the *resonating* wave by use of line-narrowing elements. The linewidth of the complementary *nonresonating* wave can be much broader if, for example, the bandwidth of the pump is broad.

A narrow-linewidth SRO allows certain tolerance from the viewpoint of the bandwidth of the pump source. This tolerance is determined by the OPO acceptance bandwidth with respect to the pump wavelength variations at a fixed signal or idler wave. A large acceptance bandwidth may result in a simpler design of the first-stage OPO, since it is no longer necessary to have a narrow-linewidth pump.

We have chosen type II phase matching for our narrow-linewidth ZGP OPO. Figure 2(a) shows theoretical type II angle tuning curves, as well as calculated acceptance bandwidths with respect to the pump (near 2.55 μm) for ZGP type II and for resonating (and fixed) signal [Fig. 2(b)] or for resonating (and fixed) idler [Fig. 2(c)] waves. For ZGP dispersion relations, we have used the most recent Sellmeier equations of Zelmon *et al.*[13] One can see from Fig. 2 that relatively broad acceptance bandwidths for the pump pulse wavelength ($\Delta \nu_{pu}$) exist in the whole tuning range of the signal (3.5–4.8 μm, $\Delta \nu_{pu} > 18$ cm^{-1}) and of the idler (5.5–10.5 μm, $\Delta \nu_{pu} > 100$ cm^{-1}).

3. LiNbO$_3$ OPO PUMP SOURCE

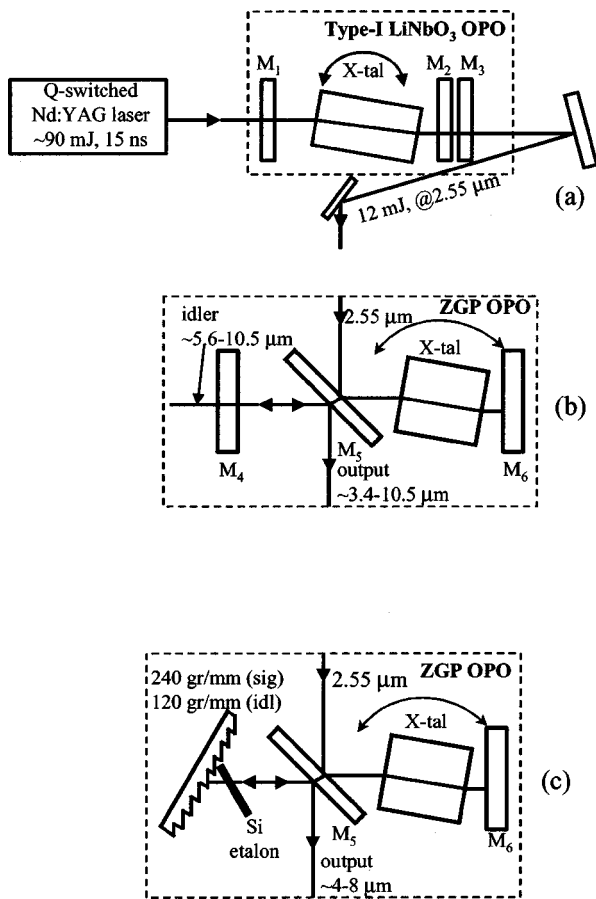We used a type I LiNbO$_3$ crystal (35-mm long, cut at 46.9°) for the first-stage OPO pumped at 1.064 μm. The

Fig. 1.   Layout of the tandem mid-IR OPO. (a) $LiNbO_3$ OPO. Mirrors M_1 and M_2 have HR for signal wave (1.5–2 μm) and HT for pump (1.064 μm) and idler (2.2–3.6 μm) waves. Mirror M_3 is used for pump recycling and has HR at 1.064 μm and HT at signal and idler waves. (b) Simple ZGP OPO configuration. Mirror M_4 has HR at signal wavelengths (3.3–4.8 μm) and HT for idler wavelengths (5.3–10.5 μm).   Mirror M_5 has HR at 2.55 μm and HT (> 80%) for both signal and idler wavelengths. M_6 is a gold mirror with HR for all the three waves. (c) Narrow-linewidth ZGP OPO that uses a diffraction grating (blazed at 3.2 μm or at 6.4 μm) and an etalon.

$LiNbO_3$ SRO cavity shown in Fig. 1(a) consisted of two plane-parallel mirrors, M_1 and M_2, separated by 5 cm, highly reflective (HR) for the signal wave and highly transmissive (HT) for the idler.   We used an additional high reflector mirror, M_3, for the pump 1.064-μm beam recycling.   When the $LiNbO_3$ OPO was pumped with 90-mJ, 15-ns pulses at 1.064 μm (linewidth <1 cm^{-1}), the idler pulse energy at 2.55 μm was 12 mJ (pulse-to-pulse stability 5%), the measured linewidth was 15 cm^{-1} FWHM, and the pulse duration was 12 ns (the 2.55-μm wavelength was chosen as a trade-off between the narrower spectrum far from degeneracy and higher energy close to degeneracy at 2.13 μm).   The beam profile at 2.55 μm was slightly elliptical, with the $1/e^2$ beam radius w_x = 2 mm (p-plane), w_y = 1.5 mm (s-plane), and the beam quality factor was measured to be $M^2 \approx 2.5$.

4. ZGP OPO PUMPED AT 2.55 μm

To obtain the main ZGP OPO output characteristics, we first used a simple SRO configuration shown in Fig. 1(b).

Mirror M_4 served as an output coupler for the idler beam and was highly reflective (R > 95%) at the signal wave (3.3–4.8 μm) and highly transmissive (T > 80%) at the idler (5.3–10.5 μm).   Mirror M_5 (HR at pump and HT at signal and idler) was used to couple the 2.55-μm pump into the cavity.   The gold mirror, M_6, served as a high reflector (R = 98%) for all three (pump, signal, and idler) waves.   The OPO cavity physical length was 5.5 cm.

We used an INRAD-grown ZGP crystal 4 mm × 8 mm × 14 mm in size.   The crystal was grown by the horizontal gradient freeze technique and subsequently was annealed at low temperatures to reduce residual linear absorption at λ = 2–3 μm.[3]   The crystal was oriented with backreflection Laue optics and a double-crystal x-ray spectrometer and cut at θ = 70° (φ = 45°) for type II phase-matching.   The effective nonlinearity at this crystal orientation is $d_{eff} = d_{36} \sin\theta \sin 2\varphi \approx 70$ pm/V.   A broadband antireflection (AR) coating was deposited onto the crystal to reduce reflection losses to ~1% per face at signal and pump wavelengths (at the idler wavelength the AR coating was not optimized, so that reflection losses were 5–10% per face).

The pump beam at 2.55 μm was left unfocused [w_x = 2.1 mm (p plane) and w_y = 1.7 mm at the ZGP surface] and the maximum power density at the ZGP crystal surface was ~25 MW/cm^2.   For the basic OPO configuration described the oscillation threshold was measured to be 3.5 MW/cm^2 (fluence 0.04 J/cm^2).   The threshold fluence is close (to within 25%) to the value obtained for a type II ZGP OPO that was pumped by a narrow-linewidth Er laser at 2.8 μm.[6]   This fact indirectly confirms that our pump bandwidth at 2.55 μm is within the pump wavelength acceptance bandwidth of ZGP.   At a pump energy of 12 mJ, the idler energy (coming through M_4)
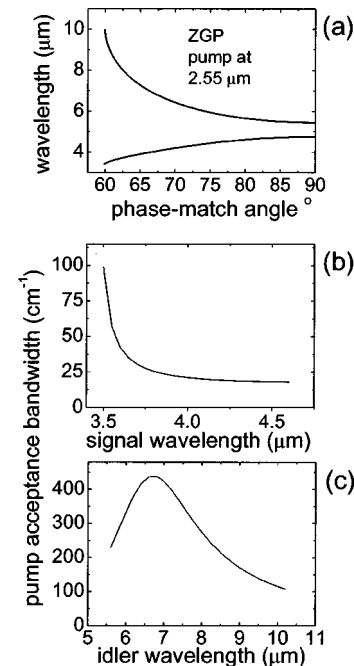

Fig. 2.   (a) Theoretical ZGP type II angle tuning curves.   Wavelength dependence of acceptance bandwidths with respect to the pump (near 2.55 μm) for (b) resonating and fixed signal and (c) for resonating and fixed idler.   We assumed L(ZGP) = 14 mm.
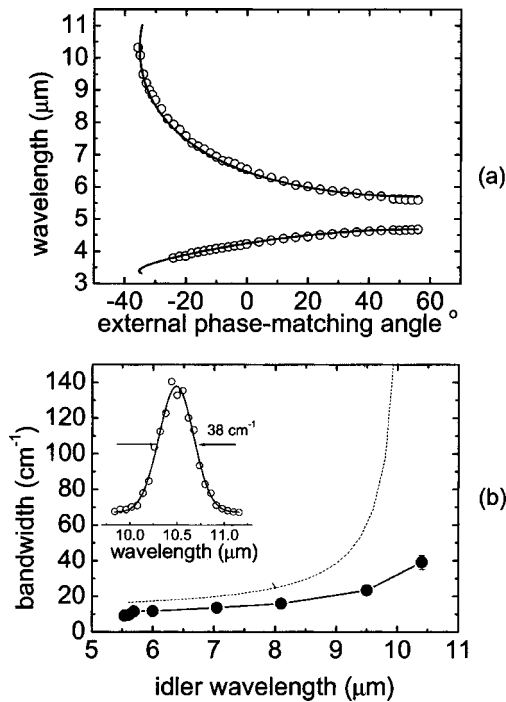
Fig. 3. (a) Experimental type II OPO tuning curve (open circles) with respect to the tilt angle of ZGP (cut at $\theta_0 = 70°$). Theoretical tuning curves (solid curves) were calculated by using the Sellmeier equations of Zelmon *et al.*[13] (b) Idler pulse bandwidth versus wavelength. Dashed line: calculated OPO gain bandwidth. Inset: idler pulse spectrum near $\lambda = 10.5\,\mu$m.
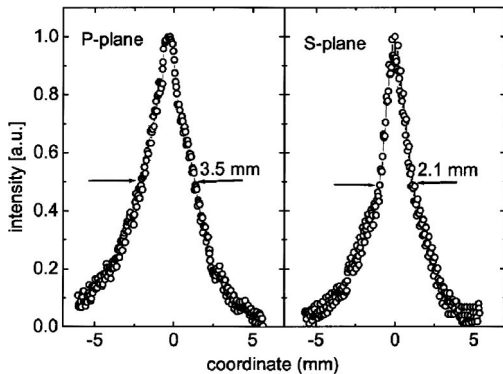

Fig. 4. Spatial profile of the $\lambda = 6.7\,\mu$m idler beam detected at the distance of 75 cm from the OPO.

reached 0.5 mJ (at $\lambda = 6.7\,\mu$m), which corresponds to a conversion efficiency of 4% and a quantum conversion efficiency of $\sim 10\%$.

Experimental angular (with respect to external angle) tuning curves for a type II OPO are presented in Fig. 3(a) along with theoretical tuning curves obtained using data from Ref. 13. Figure 3(b) shows the OPO output bandwidth as a function of the idler wavelength. This bandwidth correlates with the calculated gain bandwidth of the OPO [dashed line in Fig. 3(b)] but is smaller owing to the multipass action of the OPO cavity. With the fixed set of optics, we were able to generate wavelengths in the range of 3.4–10.5 μm with the exception of a gap in the 4.7–5.6 μm region. The idler pulse spectrum at 10.5 μm (FWHM = 38 cm^{-1}) is shown in the inset to Fig. 3(b).

For the idler beam at $\lambda = 6.7\,\mu$m, the *p*-plane and *s*-plane FWHM divergence was 4.7 and 2.8 mrad, respectively, as deduced from the spatial profile detected with a Spiricon linear pyroelectric array at a distance of 75 cm from the OPO (Fig. 4). This corresponds to beam quality factors, $M_x^2 \approx 4$ (*p*-plane) and $M_y^2 \approx 1.9$ (*s*-plane).

5. NARROW-LINEWIDTH ZGP OPO

To achieve a narrow linewidth, we used an intracavity diffraction grating at the Littrow angle or a combination of a diffraction grating and an etalon [Fig. 1(c)]. We used either a 240 grooves/mm grating (blazed at 3.2 μm) in the SRO cavity to oscillate on the signal wave or a 120 grooves/mm grating (blazed at 6.4 μm) for oscillating on the idler wave. Taking into account diffraction (first-order diffraction is assumed), aperture effects, and the number of passes in the OPO cavity, our estimate of the output linewidth of the resonated signal wave for an OPO containing a grating, according to the formulas (47) and (48) given by Brosnan and Byer,[14] gives 1.2–1.5 cm^{-1} at $\lambda \sim 4\,\mu$m.

Figures 5(a) and 5(b) show output spectra of the ZGP OPO near $\lambda = 4.3\,\mu$m and 6.8 μm. Filled circles correspond to the OPO configuration with no spectral-narrowing elements inside the cavity. The spectra were detected with a scanning 27.5 cm spectrograph (ARC
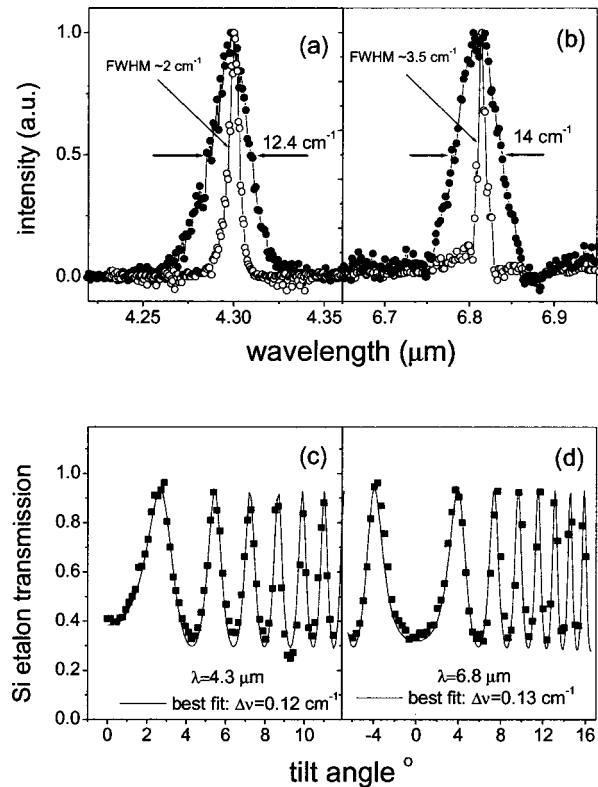

Fig. 5. Output spectra of the ZGP OPO (a) near $\lambda = 4.3\,\mu$m and (b) 6.8 μm. Filled circles, no spectral-narrowing elements inside the OPO cavity; open circle, with a diffraction grating inside the cavity. Transmission interferograms (filled squares) of the output of the OPO containing both a grating and an etalon (c) near $\lambda = 4.3\,\mu$m and (d) 6.8 μm, passing through a 2-mm-thick Si etalon. Solid curves represent calculated results with the best-fit linewidths of 0.12 cm^{-1} and 0.13 cm^{-1}, respectively.
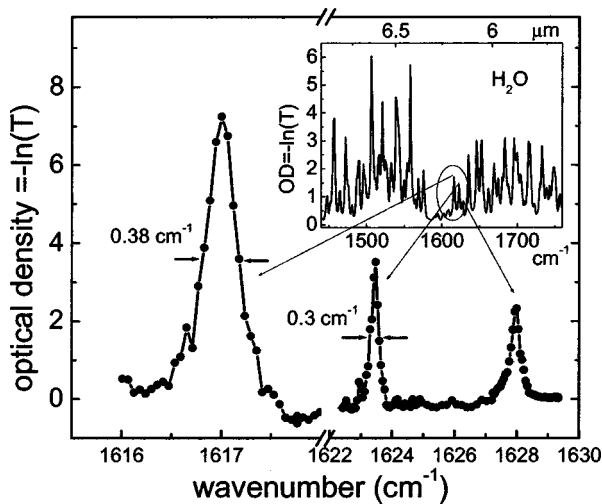
Fig. 6. Water vapor absorption spectrum (at saturated pressure at 60 °C in a cell length of 15 cm) taken near $\lambda = 6.2\,\mu$m with a narrow-linewidth ZGP OPO. Inset, absorption spectrum obtained with FTIR spectrometer (2 cm^{-1} resolution).

Spectra Pro 275) with an attached linear pyroelectric array detector (Spiricon; 256 pixels, 100 μm/pixel). The estimated system resolution varies from 1.5 to 3 cm^{-1} in the 4–10 μm wavelength range. One can see from Fig. 5 that introducing a diffraction grating gives a noticeable line narrowing, down to the limit of spectral resolution of the monochromator-plus-linear-array system.

Further reduction of the output linewidth was accomplished by addition of an intracavity etalon inside the OPO cavity [Fig. 1(c)]. The etalons used in our study were uncoated plane-parallel Si plates ($n = 3.42$) of different thickness. In this case we get an etalon finesse value ~2.6 for the mid-IR wavelengths. For a 1-mm thick Si etalon, for example (free spectral range 1.5 cm^{-1}), it is easy to estimate that the etalon resonant transmission peaks have FWHM of ~0.5 cm^{-1}. By properly choosing the etalon tilt angle with respect to the intracavity beam and etalon thickness, one can get the OPO oscillating within a single etalon resonance peak. Calculations that take into account linewidth narrowing due to multiple roundtrips of the resonated wave show that, in the case of the OPO with the grating, insertion of a Si etalon with a thickness from 1 to 2 mm results in an output linewidth of 0.1–0.15 cm^{-1}. Using Si etalons thicker than 2 mm is not practical, since the spacing between resonant peaks (free spectral range) becomes less than the gain profile set by the nonlinear crystal and the grating; this results in an OPO oscillating simultaneously at two resonant etalon peaks.

Experimentally, to estimate the linewidth of the linewidth-narrowed OPO, we used a separate, uncoated Si etalon that was placed outside the OPO cavity. The OPO beam was sent through the Si etalon and the corresponding transmitted intensity was detected as a function of the etalon tilt angle. Interferograms obtained in this way were fitted theoretically to the linewidth of the OPO radiation as the only varying parameter. It is clear that narrower OPO linewidths correspond to larger amplitudes of the transmission oscillations. Experimental transmission interferograms along with best-fit curves

are shown in Figs. 5(c) and 5(d) for the OPO with a grating and a 2-mm-thick intracavity etalon. The linewidth was measured to be 0.12 cm^{-1} at the resonating signal (near $\lambda = 4.3\,\mu$m) and 0.13 cm^{-1} at the resonating idler wave (near $\lambda = 6.8\,\mu$m). This linewidth was obtained at the full pump energy (3–5 times the OPO threshold) and corresponds to approximately 3 axial modes of the OPO cavity. Oscillations of the transmitted intensity, similar to those of Figs. 5(c) and 5(d), can also be obtained when the angle of the Si etalon, placed outside the OPO cavity, is fixed, but the OPO frequency is fine tuned.

To demonstrate the usefulness of our narrow-linewidth OPO system for molecular detection, we measured the absorption spectrum of water vapor near $\lambda = 6.2\,\mu$m at saturated pressure at 60 °C in a cell length of 15 cm. The linewidths of the rotational–vibrational spectrum of 0.3–0.4 cm^{-1} (Fig. 6), which we obtained using an OPO with a 120 grooves/mm grating and a 1-mm-thick intracavity etalon, are in good accord with the linewidths obtained from the HITRAN96 database. The inset in Fig. 6 shows, for comparison, the water vapor absorption spectrum obtained with Fourier transform infrared spectrometer with a 2-cm^{-1} resolution.

For the cavity layout with a grating and an etalon, pulse energies in the range of 200–10 μJ (pulse-to-pulse stability 10%), were available across the tuning range of 3.8–8 μm. This tuning range was smaller than in the case of Fig. 1(b) because of the decrease in the diffraction grating efficiency at longer waves, far from the blazing wavelength (6.4 μm). Also, the smaller efficiency at the resonating idler wave is the result of nonoptimal AR coating of ZGP crystal for the idler wavelength.

6. CONCLUSION

We have demonstrated, for the first time, a narrow-linewidth ZGP-crystal-based OPO. The OPO was pumped at 2.55 μm and was tunable in the mid-IR from 3.7 to 8 μm with output energies in the range of 200–10 μJ and linewidths of approximately 0.1 cm^{-1}, corresponding to ~3 axial OPO cavity modes. Further reduction of the linewidth to one axial mode ($\Delta\nu \sim 10^{-3}$–10^{-4} cm^{-1}) would be possible with a higher finesse (~30) intracavity etalon. The above tuning range can be extended to 10.5 μm by a proper choice of diffraction gratings. Finally, we have shown that a broadband pump can be used to achieve a narrow-linewidth OPO output.

*Present address, Bell Laboratories, Lucent Technologies, 600 Mountain Avenue, Murray Hill, New Jersey 07974; or e-mail fganikhanov@lucent.com.

†Present address, Informed Diagnostics, Inc., 1050 East Duane Avenue, Suite I, Sunnyvale, California 94086; or e-mail kvodopyanov@infodiag.com.

REFERENCES

1. D. N. Nikogosyan, *Properties of Optical and Laser-Related Materials. A Handbook* (Wiley, Chichester, 1997), pp. 133–140.
2. P. G. Schunemann, P. A. Budni, L. Pomeranz, M. G. Knights, T. M. Pollak, and E. P. Chicklis, "Improved $ZnGeP_2$ for high power OPO's," in *Advanced Solid State Lasers*, C. R. Pollock and W. R. Bosenberg, eds., Vol. 10 of OSA Trends in Optics and Photonics Series (Optical Society of America, Washington D.C., 1997), pp. 253–255.
3. I. Zwieback, J. Maffetone, and W. Ruderman, "Growth of high quality $ZnGeP_2$ single crystals," Naval Research Laboratory, Contract No. N00014-94-C-6207, Final Report INRAD, Northvale, N.J., 1995.
4. T. Allik, S. Chandra, D. M. Rines, P. G. Schunemann, J. A. Hutchinson, and R. Utano, "Tunable 7–12-μm optical parametric oscillator using a Cr, Er:YSGG laser to pump CdSe and $ZnGeP_2$ crystals," Opt. Lett. **22**, 597–599 (1997).
5. P. A. Budni, L. A. Pomeranz, M. L. Lemons, P. G. Schunemann, T. M. Pollak, and E. P. Chicklis, "10 W mid-IR holmium pumped $ZnGeP_2$ OPO," in *Advanced Solid State Lasers*, W. R. Bosenberg and M. M. Fejer, eds., Vol. 19 of OSA Trends in Optics and Photonics Series (Optical Society of America, Washington D.C., 1998), pp. 90–92.
6. J. A. C. Terry, K. J. McEwan, and M. J. P. Payne, "A tandem OPO route to the mid-IR," in *Advanced Solid State Lasers*, W. R. Bosenberg and M. M. Fejer, eds., Vol. 19 of OSA Trends in Optics and Photonics Series (Optical Society of America, Washington D.C., 1998), pp. 99–101.
7. P. B. Phua, K. S. Lai, R. F. Wu, and T. C. Chong, "Coupled tandem optical parametric oscillator (OPO): an OPO within an OPO," Opt. Lett. **23**, 1262–1264 (1998).
8. E. Cheung, S. Palese, H. Injeyan, C. Hoefer, J. Ho, R. Hilyard, H. Komine, J. Berg, and W. Bosenberg, "High-power conversion to mid-IR using KTP and ZGP OPOs," in *Advanced Solid-State Lasers*, M. M. Fejer, H. Injeyan, and U. Keller, eds., Vol. 26 of OSA Trends in Optics and Photonics Series (Optical Society of America, Washington D.C., 1999), pp. 358–361.
9. K. L. Vodopyanov, F. Ganikhanov, J. P. Maffetone, I. Zwieback, and W. Ruderman, "$ZnGeP_2$ optical parametric oscillator with 3.8–12.4-μm tunability," Opt. Lett. **25**, 841–843 (2000).
10. P. A. Budni, L. A. Pomeranz, M. L. Lemons, C. A. Miller, J. R. Mosto, and E. P. Chicklis, "Efficient mid-infrared laser using 1.9-μm-pumped Ho:YAG and $ZnGeP_2$ optical parametric oscillator," J. Opt. Soc. Am. B **17**, 723–728 (2000).
11. K. L. Vodopyanov, "Parametric generation of tunable infrared radiation in $ZnGeP_2$ and GaSe pumped at 3 μm," J. Opt. Soc. Am. B **10**, 1723–1729 (1993).
12. V. Petrov, F. Rotermund, F. Noack, and P. Schunemann, "Femtosecond parametric generation in $ZnGeP_2$," Opt. Lett. **24**, 414–416 (1999).
13. D. E. Zelmon, E. A. Hanning, and P. Schunemann, "Refractive index measurement and new Sellmeier coefficients of zinc germanium phosphide (ZnGeP2) from 2–9 microns with implications for phase matching in optical parametric oscillators," in *Infrared Applications of Semiconductors III, Vol. 607 of MRS Symposium Proceedings*, M. O. Manesreh, B. J. H. Stadler, I. Ferguson, and Y.-H. Zhang, eds. (Materials Research Society, Pittsburgh, Pa., 2000), pp. 451–456 (2000).
14. S. J. Brosnan and R. L. Byer, "Optical parametric oscillation threshold and linewidth studies," IEEE J. Quantum Electron. **QE-15**, 415–431 (1979).